

Huge light scattering from active anisotropic spherical particles

Xiaofeng Fan,^{1,*} Zexiang Shen,¹ and Boris Luk'yanchuk^{2,3}

¹ School of Physical and Mathematical Sciences, Nanyang Technological University, Singapore 637616

² Data Storage Institute, DSI Building, 5 Engineering Drive 1, Singapore, 117608

³ Boris.L@dsi.a-star.edu.sg

* xffan@ntu.edu.sg

Abstract: The light scattering by a spherical particle with radial anisotropic permittivity ϵ and permeability μ are discussed in detail by expanding Mie theory. With the modified vector potential formulation, the electric anisotropy effects on scattering efficiency are addressed by studying the extinction, scattering, absorption and radar cross sections following the change of the transverse permittivity ϵ_t , the longitudinal permittivity ϵ_r and the particle size q . The huge scattering cross sections are shown by considering the possible coupling between active medium and plasmon polaritons and this will be possible to result in spaser from the active plasmons of small particle.

© 2010 Optical Society of America

OCIS codes: (240.6680) Surface plasmons; (260.3910) Metal optics; (290.4020) Mie Theory; (140.3380) Laser Materials.

References and links

1. M. L. Brongersma and P. G. Kik, *Surface plasmon nanophotonics* (Springer Series in Optical Sciences, Springer, 2007), Vol. 131.
2. S. A. Maier, *Plasmonics: fundamentals and applications* (Springer, 2007).
3. B. Luk'yanchuk, N. I. Zheludev, S. A. Maier, N. J. Halas, P. Nordlander, H. Giessen, and C. T. Chong, "The Fano resonance in plasmonic nanostructures and metamaterials," *Nat. Mater.* **9**, 707-715 (2010).
4. P. Muhlschlegel, H.-J. Eisler, O. J. F. Martin, B. Hecht, and D. W. Pohl, "Resonant optical antennas," *Science* **308**, 1607-1608 (2005).
5. J. A. Gordon, and R. W. Ziolkowski, "The design and simulated performance of a coated nano-particle laser," *Opt. Express* **15**, 2622-2653 (2007).
6. S. Noda, "Seeking the ultimate nanolaser," *Science* **314**, 260-261 (2006).
7. M. T. Hill, et al., "Lasing in metallic-coated nanocavities," *Nature Photon.* **1**, 589-594 (2007).
8. C. Genet and T. W. Ebbesen, "Light in tiny holes," *Nature* **445**, 39-46 (2007).
9. B. Liedberg, C. Nylander, and I. Lundstrom, "Surface plasmon resonance for gas detection and biosensing," *Sens. Actuators* **4**, 299-304 (1983).
10. C. A. Mirkin, R. L. Letsinger, R. C. Mucic, and J.J. Storhoff, "A DNA-based method for rationally assembling nanoparticles into macroscopic materials," *Nature* **382**, 607-609 (1996).
11. A. J. Haes, L. Chang, W. L. Klein, and R. P. Van Duyne, "Detection of a biomarker for alzheimer's disease from synthetic and clinical samples using a nanoscale optical biosensor," *J. Am. Chem. Soc.* **127**, 2264-2271(2005).
12. T. Rindzevicius, Y. Alaverdyan, A. Dahlin, F. Hook, D. S. Sutherland, M. Kall, "Plasmonic sensing characteristics of single nanometric holes," *Nano Lett.* **5**, 2335-2339 (2005).
13. S. Nie and S. R. Emony, "Probing single molecules and single nanoparticles by surface-enhanced Raman scattering," *Science* **275**, 1102-1106 (1997).
14. J. P. Kottmann and O. J. F. Martin, "Plasmon resonant coupling in metallic nanowires," *Opt. Express* **8**, 655-663 (2001).
15. P. Bharadwaj, P. Anger, and L. Novotny, "Nanoplasmonic enhancement of single-molecule fluorescence," *Nanotechnology* **18**, 044017 (2007).

16. Y. Fu, J. Zhang, and J.R. Lakowicz, "Plasmon-enhanced fluorescence from single fluorophores end-linked to gold nanorods," *J. Am. Chem. Soc.* **132**, 5540-5541 (2010).
17. P. Andrew, and W. L. Barnes, "Energy transfer across a metal film mediated by surface plasmon polaritons," *Science* **306**, 1002-1005 (2004).
18. P. Andrew, and W.L. Barnes, "Förster energy transfer in an optical microcavity," *Science* **290**, 785-788 (2000).
19. E. Prodan, C. Radloff, N. J. Halas, and P. Nordlander, "A hybridization model for the plasmon response of complex nanostructures," *Science* **302** 419-422,(2003).
20. H. Liu and P. Lalanne, "Microscopic theory of the extraordinary optical transmission," *Nature* **452**, 728-731 (2008).
21. R. F. Oulton, V. J. Sorger, D. A. Genov, D. F. P. Pile, and X. Zhang, "A hybrid plasmonic waveguide for sub-wavelength confinement and long-range propagation," *Nat. Photonics* **2**, 496-500 (2008)
22. M. Nezhad, K. Tetz, and Y. Fainman, "Gain assisted propagation of surface plasmon polaritons on planar metallic waveguides," *Opt. Express* **12**, 4072-4079 (2004)
23. N. M. Lawandy, "Localized surface plasmon singularities in amplifying media," *Appl. Phys. Lett.* **85**, 5040-5042 (2004).
24. M. A. Noginov, G. Zhu, M. Bahoura, J. Adegoke, C. E. Small, B. A. Ritzo, V. P. Drachev, and V. M. Shalaev, "Enhancement of surface plasmons in an Ag aggregate by optical gain in a dielectric medium," *Opt. Lett.* **31**, 3022-3024 (2006).
25. J. Seidel, S. Grafstrom, and L. Eng, "Stimulated emission of surface plasmons at the interface between a silver film and an optically pumped dye solution," *Phys. Rev. Lett.* **94**, 177401 (2005).
26. M. A. Noginov, V. A. Podolskiy, G. Zhu, M. Mayy, M. Bahoura, J. A. Adegoke, B. A. Ritzo, and K. Reynolds, "Compensation of loss in propagating surface plasmon polariton by gain in adjacent dielectric medium," *Opt. Express* **16**, 1385-1392 (2008).
27. D. J. Bergman and M. I. Stockman, "Surface plasmon amplification by stimulated emission of radiation: quantum generation of coherent surface plasmons in nanosystems," *Phys. Rev. Lett.* **90**, 027402 (2003).
28. M. A. Noginov, G. Zhu, A. M. Belgrave, R. Bakker, V. M. Shalaev, E. E. Narimanov, S. Stout, E. Herz, T. Suteewong, and U. Wiesner, "Demonstration of a spaser-based nanolaser," *Nature* **460**, 1110-1112 (2009).
29. M.I. Stockman, "Spasers explained," *Nat. Photonics* **2**, 327-329 (2008).
30. J. B. Pendry, "Negative refraction makes a perfect lens," *Phys. Rev. Lett.* **85**, 3966-3969 (2000).
31. E. Prodan and P. Nordlander, "Plasmon hybridization in spherical nanoparticles," *J. Chem. Phys.* **120**, 5444-5454 (2004)
32. R. D. Graglia, P. L. E. Uslenghi, and R. S. Zich, "Moment method with isoparametric elements for three-dimensional anisotropic scatterers," *Proc. IEEE* **77**, 750-760 (1989).
33. J. I. Dadap, J. Shan, K. B. Eisenthal, and T. F. Heinz, "Second-Harmonic Rayleigh scattering from a sphere of centrosymmetric material," *Phys. Rev. Lett.* **83**, 4045-4048 (1999).
34. V. V. Varadan, A. Lakhtakia, and V. K. Varadan, "Scattering by three-dimensional anisotropic scatterers," *IEEE Trans. Antennas Propag.* **37**, 800-802 (1989).
35. Y. L. Geng, X. B. Wu, L. W. Li, and B. R. Guan, "Mie scattering by a uniaxial anisotropic sphere," *Phys. Rev. E* **70**, 056609 (2004).
36. B. Stout, M. Neviere, and E. Popov, "Mie scattering by an anisotropic object. Part I: Homogeneous sphere," *J. Opt. Soc. Am. A* **23**, 1111-1123 (2006).
37. B. Stout, M. Neviere, and E. Popov, "Mie scattering by an anisotropic object. Part II: Arbitrary-shaped object differential theory," *J. Opt. Soc. Am. A* **23**, 1124-1134 (2006).
38. C.-W. Qiu, L. W. Li, T.-S. Yeo, and S. Zouhdi, "Scattering by rotationally symmetric anisotropic spheres: Potential formulation and parametric studies," *Phys. Rev. E* **75**, 026609 (2007).
39. B. S. Luk'yanchuk, and C.-W. Qiu, "Enhanced scattering efficiencies in spherical particles with weakly dissipating anisotropic materials," *Appl. Phys. A* **92**, 773 (2008)
40. M. Born and E. Wolf, *Principles of optics, 7th ed.* (Cambridge University Press, Cambridge, 1999).
41. Edward J. Rothwell and Michael J. Cloud, *Electromagnetics, 2nd ed.* (CRC Press, Taylor & Francis Group, 2009).
42. W. C. Chew, *Waves and fields in inhomogeneous media* (Van Nostrand, New York, 1990).
43. W. Ren, "Contributions to the electromagnetic wave theory of bounded homogeneous anisotropic media," *Phys. Rev. E* **47**, 664-673 (1993).
44. C. T. Tai, *Dyadic Green's functions in electromagnetic theory, 2nd ed.*(IEEE Press, Piscataway, NJ, 1994).
45. A. L. Aden, and M. Kerker, "Scattering of electromagnetic waves from two concentric spheres," *J. Appl. Phys.* **22**, 1242-1246 (1951).
46. Z. S. Wu and Y. P. Wang, "Electromagnetic scattering for multilayered sphere: Recursive algorithms," *Radio Sci.* **26**, 1393-1401(1991).
47. R. J. Tarento, K. H. Bennemann, P. Joyes, and J. Van de Walle, "Mie scattering of magnetic spheres," *Phys. Rev. E* **69**, 026606 (2004).
48. P. W. Barber and S. C. Hill, *Light scattering by particles: computational methods* (World Scientific, Singapore, 1990).

49. C. F. Bohren and D. R. Huffman, *Absorption and scattering of light by small particles* (Wiley, New York, 1983).
 50. M. I. Tribelsky and B. S. Luk'yanchuk, "Anomalous light scattering by small particles," *Phys. Rev. Lett.* **97**, 263902 (2006).
 51. B. S. Luk'yanchuk, M. I. Tribelsky, Z. B. Wang, Y. Zhou, M. H. Hong, L. P. Shi, and T. C. Chong, "Extraordinary scattering diagram for nanoparticles near plasmon resonance frequencies," *Appl. Phys. A* **89**, 259-264 (2007).
 52. M. I. Tribelsky, "Anomalous light absorption by small particles," arXiv:0912.3644v1.
-

1. Introduction

Controlling light energy into nanometer scale is one of the rapidly growing fields of material physics and nanotechnology[1, 2, 3] which hosts a lot of important research directions with potential applications such as high-resolution optical imaging[4, 5], small-scale sensing techniques[7, 8], and numerous biomedical applications[9, 10, 11, 12]. Presently, designing the metal/dielectric interface with the use of surface plasmon polaritons is considered to be an effective approach of manipulating light on nano scale. With the isolated small metal particle, the local electromagnetic field can be enhanced by the surface plasmons localized on the surface and thus be utilized to enhance Raman scattering[13, 14], fluorescence of single molecule[15, 16] and transfer resonantly the energy of exciton[17], and so on. With designing the proper periodic pattern on metal materials or the interface of active medium, dielectric and metal, the different plasmon modes can be hybridized and tune the resonance frequency for guiding electromagnetic wave on nanosized structure[18, 19, 20, 21] and lasing of semiconductor nano particle or fluorescence molecules in dielectric media with assistance of plasmons[22, 23, 24, 25, 26, 27, 28, 29]. Therefore, the anisotropic materials or designed metamaterials with anisotropy have been a subject of great interest, since the merging of plasmonics and these materials may open up a new perspective to control the electromagnetic wave, such as the achievement of negative index metamaterials in the optical frequencies[30].

Prodan *et al.* have studied the plasmon hybridization of complex nanoshell structures with a metallic shell and a dielectric core[31, 19]. The interaction of bare plasmon modes of individual surface is demonstrated. Furthermore, Bergman *et al.* predicted that the surface plasmon can be amplified by stimulated emission of radiation and thus result in lasing with the generator of coherent surface plasmons[27]. Recently, it was experimentally demonstrated that the spaser is realized on a conjugate structure with a metallic core and a dye-doped dielectric shell which is as an active medium to overcome the inherent loss of surface plasmon inside metal core[28]. In this paper, we study the fancy effect of light scattering on the small particles with radial anisotropic permittivity. Some progress has been made in this direction about spherical anisotropic structures[32, 33, 34, 35, 36, 37, 38, 39]. The method of moments, coupled-dipole methods, second-harmonic generation approach and expanded Mie theory have been developed to expand the field expressions[32, 33, 34, 36]. Some new effects of light scattering by anisotropic materials, such as the additional increase in field enhancement near surface plasmon resonance frequencies induced by anisotropy, have been analyzed[39]. Here, with modified Mie theory, we will analyze the space of parameters including the transverse permittivity ϵ_t , the longitudinal permittivity ϵ_r , the particle size a and wavelength of incident wave λ . We consider the anisotropy of permittivity ϵ results in the spherical particles have different properties in different directions, such as metallic property and light-active dielectric property. The huge light scattering is found in special region of parameter space after inspecting the extinction, scattering, absorption and radar cross section. This fantastic effect is suspected to be due to the coupling between active medium and plasmons and be possible to result in spaser.

2. Theoretical model

Different analytical methods have been developed to deal with the light scattering with medium with different structures[40, 41]. For planar multilayered structures, the 3D Fourier transform technique was usually used to relate the space and spectral domains to the analysis of the waves and fields[42, 43]. For the boundary-value problems and periodic structures, the Green's functional technique as a kernel is used to solve the integral equation[44]. For the spherical and cylindrical structures, the Lorenz-Mie approach is a powerful method of separation of variables to expand angularly the electromagnetic field[45, 46, 47, 48, 49]. Here, we chose to modify the Mie theory to deal with the particle with radial anisotropy[38, 40].

We assume that the plane wave with the electric field polarized along the x axis is scattered by the particle immersed in homogeneous medium. Considering the scattering about monochromatic wave, the time dependence $e^{-i\omega t}$ part can be suppressed and the electric and magnetic vectors satisfy the time-free Maxwell's equations:

$$\nabla \vec{H} = -ik_0 \varepsilon \cdot \vec{E} \text{ and } \nabla \vec{E} = ik_0 \mu \cdot \vec{H}, \quad (1)$$

where k_0 is the wave vector of light in vacuum. The uniaxial anisotropy of particle is defined by the constitutive tensors of the permittivity and permeability as:

$$\varepsilon = \begin{pmatrix} \varepsilon_r & 0 & 0 \\ 0 & \varepsilon_t & 0 \\ 0 & 0 & \varepsilon_t \end{pmatrix} \text{ and } \mu = \begin{pmatrix} \mu_r & 0 & 0 \\ 0 & \mu_t & 0 \\ 0 & 0 & \mu_t \end{pmatrix} \quad (2)$$

where the coordinate system is spherical coordinate, and ε_r , ε_t , μ_r and μ_t are the longitudinal permittivity, transverse permittivity, longitudinal permeability and transverse permeability, respectively. In general case, these four values ε_r , ε_t , μ_r and μ_t will be complex numbers, i.e. $\varepsilon_r = Re[\varepsilon_r] + i Im[\varepsilon_r]$, $\varepsilon_t = Re[\varepsilon_t] + i Im[\varepsilon_t]$, etc. As usual, the electric and magnetic vectors can be expressed by the Debye's scalar potentials Π_{TE} and Π_{TM} . Thus, the Maxwell vector equations are transferred as the scalar equations about the magnetic Π_{TE} and electric Π_{TM} potentials, which are expressed as:

$$\frac{\varepsilon_r}{\varepsilon_t} \frac{\partial^2 \Pi_{TM}}{\partial r^2} + \frac{1}{r^2 \sin \theta} \frac{\partial}{\partial \theta} \left(\sin \theta \frac{\partial \Pi_{TM}}{\partial \theta} \right) + \frac{1}{r^2 \sin^2 \theta} \frac{\partial^2 \Pi_{TM}}{\partial \varphi^2} + k_0^2 \varepsilon_r \mu_t \Pi_{TM} = 0, \quad (3)$$

$$\frac{\mu_r}{\mu_t} \frac{\partial^2 \Pi_{TE}}{\partial r^2} + \frac{1}{r^2 \sin \theta} \frac{\partial}{\partial \theta} \left(\sin \theta \frac{\partial \Pi_{TE}}{\partial \theta} \right) + \frac{1}{r^2 \sin^2 \theta} \frac{\partial^2 \Pi_{TE}}{\partial \varphi^2} + k_0^2 \varepsilon_t \mu_r \Pi_{TE} = 0, \quad (4)$$

for the scattering by particle with anisotropic permittivity ε and permeability μ . Solving these equations with corresponding boundary conditions, the scattering amplitudes B_l^e (electric) and B_l^m (magnetic) can be found to be as:

$$B_l^e = i^{l+1} \frac{2l+1}{l(l+1)} b_l^e \text{ and } B_l^m = i^{l+1} \frac{2l+1}{l(l+1)} b_l^m, \quad (5)$$

with,

$$b_l^e = \frac{\sqrt{\varepsilon_t} \Phi_l'(k_0 a) \Phi_{v_1}(k_t a) - \sqrt{\mu_t} \Phi_l(k_0 a) \Phi_{v_1}'(k_t a)}{\sqrt{\varepsilon_t} \xi_l'(k_0 a) \Phi_{v_1}(k_t a) - \sqrt{\mu_t} \xi_l(k_0 a) \Phi_{v_1}'(k_t a)}, \quad (6)$$

$$b_l^m = \frac{\sqrt{\varepsilon_t} \Phi_l(k_0 a) \Phi_{v_2}'(k_t a) - \sqrt{\mu_t} \Phi_l'(k_0 a) \Phi_{v_2}(k_t a)}{\sqrt{\varepsilon_t} \xi_l(k_0 a) \Phi_{v_2}'(k_t a) - \sqrt{\mu_t} \xi_l'(k_0 a) \Phi_{v_2}(k_t a)}, \quad (7)$$

where $k_t = k_0 \sqrt{\epsilon_t \mu_t}$ is the wave vector in anisotropic spheres. the functions $\Phi_l(x)$ and $\xi_l(x)$ are given by

$$\Phi_l(x) = \sqrt{\frac{\pi x}{2}} J_{l+\frac{1}{2}}(x), \quad (8)$$

$$\xi_l(x) = \sqrt{\frac{\pi x}{2}} \left(J_{l+\frac{1}{2}}(x) + i N_{l+\frac{1}{2}}(x) \right) \quad (9)$$

where $J_l(x)$ and $N_l(x)$ are usual Bessel function and Neumann function. The order ν_1 and ν_2 of the spherical Bessel function Φ_{ν_1} and Φ_{ν_2} are:

$$\nu_1 = \left[l(l+1) \frac{\epsilon_t}{\epsilon_r} + \frac{1}{4} \right]^{1/2} - \frac{1}{2}, \quad (10)$$

and

$$\nu_2 = \left[l(l+1) \frac{\mu_t}{\mu_r} + \frac{1}{4} \right]^{1/2} - \frac{1}{2}. \quad (11)$$

With the solution about Π_{TE} and Π_{TM} , we can analyze the distribution of electromagnetic fields around the particle. The lost of total energy from incident wave and the energy flux due to backscattering from the particle can be also analyzed. With optical cross-section theorem, the forward scattering amplitude can be evaluated by extinction, scattering and absorption cross sections. The backward scattering amplitude can be evaluated by radar cross section. For the convenience of discussion, the dimensionless cross sections Q is introduced by the formula $Q = \sigma_{sc} / \sigma_{geom}$, where σ_{sc} is the optical cross-section of the particle and $\sigma_{geom} = \pi a^2$ is the geometrical cross section with the radius a . By the scattering amplitudes b_l^e and b_l^m , the dimensionless extinction, scattering and backscattering cross section can be expressed as:

$$\begin{aligned} Q_{ext} &= \frac{2}{k_0^2 a^2} \sum_{l=1}^{\infty} (2l+1) \text{Re}(b_l^e + b_l^m), \\ Q_{sca} &= \frac{2}{k_0^2 a^2} \sum_{l=1}^{\infty} (2l+1) [|b_l^e|^2 + |b_l^m|^2], \\ Q_{rbs} &= \frac{1}{k_0 a} \text{Re} \left| \sum_{l=1}^{\infty} (-1)^l (2l+1) (b_l^e - b_l^m) \right|^2. \end{aligned} \quad (12)$$

With the extinction and scattering cross section, the dimensionless absorption cross section can be defined by the formula, $Q_{abs} = Q_{ext} - Q_{sca}$. For discussing the light scattering due to surface plasmons, the scattering amplitudes in equ.(6)and(7) can be expressed in a more convenient form:

$$b_l^e = \frac{F_b^e(l)}{F_b^e(l) + iG_b^e(l)} \quad \text{and} \quad b_l^m = \frac{F_b^m(l)}{F_b^m(l) + iG_b^m(l)}, \quad (13)$$

with,

$$\begin{aligned} F_b^e &= \sqrt{\epsilon_t} \Phi_l'(k_0 a) \Phi_{\nu_1}(k_t a) - \sqrt{\mu_t} \Phi_l(k_0 a) \Phi_{\nu_1}'(k_t a), \\ G_b^e &= \sqrt{\epsilon_t} \chi_l'(k_0 a) \Phi_{\nu_1}(k_t a) - \sqrt{\mu_t} \chi_l(k_0 a) \Phi_{\nu_1}'(k_t a), \\ F_b^m &= \sqrt{\epsilon_t} \Phi_l(k_0 a) \Phi_{\nu_2}'(k_t a) - \sqrt{\mu_t} \Phi_l'(k_0 a) \Phi_{\nu_2}(k_t a), \\ G_b^m &= \sqrt{\epsilon_t} \chi_l(k_0 a) \Phi_{\nu_2}'(k_t a) - \sqrt{\mu_t} \chi_l'(k_0 a) \Phi_{\nu_2}(k_t a), \end{aligned} \quad (14)$$

where $\chi_l(x) = \sqrt{\frac{\pi x}{2}} N_{l+\frac{1}{2}}(x)$.

3. Results and Discussion

The special properties of surface plasmon are expected to exist in the anisotropic materials. Since the electron collective movements are shown clearly in metal, let us consider firstly the strange effect in small isotropic metallic sphere. The relative dielectric permittivity in the Drude model is described as:

$$\varepsilon_D = 1 - \frac{\omega_p^2}{\omega^2 + i\gamma\omega} \text{ with } \omega_p = \left(\frac{ne^2}{\varepsilon_0 m_0} \right)^{1/2}, \quad (15)$$

where ω_p , γ , n , e m_0 and ε_0 are the plasma frequency, frequency of electron collisions, concentration of electron, charge of electron, mass of electron and vacuum permittivity, respectively. Obviously, the value is complex, i.e. $\varepsilon_D = \text{Re}[\varepsilon_D] + i \text{Im}[\varepsilon_D]$. Here, ω_p exhibits the properties of bulk plasmons. With the decrease of size, the new plasmon modes, surface plasmons will be possible to be excited. The nondimensional quantity $q = a\sqrt{\varepsilon_m}k_0$, can be as size parameter to analyze the scattering effects with the radius of the spherical particle a and the dielectric permittivities of media ε_m . At small q , the electric dipole scattering plays the dominant role. the scattering from the magnetic amplitudes b_l^m can be also neglected. Now we consider the case which is far from the resonances. The amplitude b_l^e of electric dipole can be approximately expressed as $(-2i/3) \frac{\varepsilon_D - 1}{\varepsilon_D + 2} q^3$. This results in classical extinction efficiency $Q_{scat}^R (\simeq \frac{8}{3} |\frac{\varepsilon_D - 1}{\varepsilon_D + 2}|^2 q^4)$ of Rayleigh scattering. It should be noticed that the Q_{scat}^R has a singularity at $\varepsilon_D = -2$. Therefore, with neglecting the frequency of electron collisions ($\gamma = 0$), it is obtained that the resonance frequency of dipole surface plasmon $\omega_{sp} = \omega_p/\sqrt{3}$. By introducing normalized frequency $\omega_R = \omega/\omega_{sp}$ and normalized collision frequency $\gamma_R = \gamma/\omega_{sp}$, the Drude dielectric permittivity can be rewritten as:

$$\varepsilon_D = 1 - \frac{3}{\omega_R^2 + \gamma_R^2} + i \frac{\gamma_R}{\omega_R} \frac{3}{\omega_R^2 + \gamma_R^2}. \quad (16)$$

For the cases of weak dissipation ($\gamma_R \in [10^{-1}, 10^{-3}]$), the imaginary part of dielectric permittivity $\text{Im}[\varepsilon]$ will be less than 0.3. In the process of deducing Rayleigh formula, the $F_b^e(l)$ in denominator part of b_l^e is ignored, relative to $G_b^e(l)$. However, for the case which is near the resonances ($G_b^e(l) \rightarrow 0$), the $F_b^e(l)$ will can not be ignored. Actually, $F_b^e(l)$ corresponds to the radiative damping as shown in Refs.[50, 51]. With the consideration of radiative damping, the singularity of Rayleigh extinction efficiency will be disappeared. Meanwhile, a series of surface localized electromagnetic modes with the resonance frequencies $\omega_R(l) (\sim \sqrt{3l/(2l+1)})$ appear in the formula for small particle. This means the surface plasmons will be possible to be excited when the condition ($\text{Re}[\varepsilon_D] < -1$) is satisfied for the real part of dielectric permittivity $\text{Re}[\varepsilon_D]$ of the particle.

Under the nondissipative limit ($\text{Im}[\varepsilon_D] = 0$), the resonance extinction cross section from small particle increases with increase in the order of the resonance modes, as shown in Ref[50]. However, in the real metal materials, the different dissipative mechanisms, such as the electron-electron collision, electron-phonon coupling and electron-defect interaction, will result in the damping of the collective moving of electrons with $\text{Im}[\varepsilon_D] > 0$. With the weak dissipative damping, the resonance frequencies are not changed obviously, whereas the extinction cross section of each resonance modes will decrease quickly. As shown in Fig. 1, the decrease of the cross sections of higher order modes is quicker than that of dipole resonance cross sections.

For the particle size $q \leq 1$ with $\text{Im}[\varepsilon_D] \geq 0.07$ at each resonance frequency, the dipole resonance becomes greater than that of the higher order modes, such as quadruple. For an example, the dipole resonance of the particle with size $q = 0.5$ becomes the dominant resonance mode when the image part of permittivity ε_D is larger than 0.02. The quick decrease of cross section of high order resonance modes may be attributed to their relative small characteristic widths. As

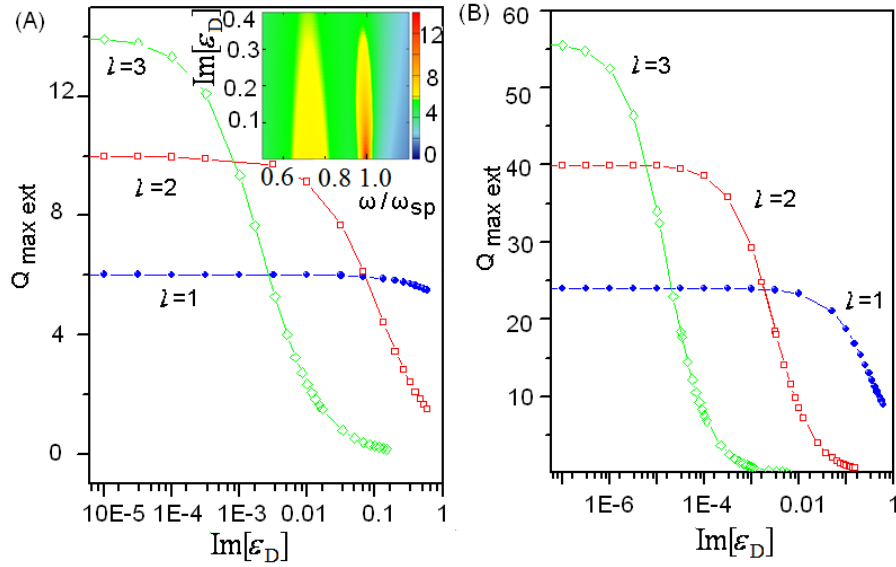


Fig. 1. The maximal value of Q_{ext} for each resonance mode as a function of the dissipative damping $Im[\epsilon_D]$ for the size $q = 1$ (A) and $q = 0.5$ (B). The Q_{ext} as a function of both frequency ω and $Im[\epsilon_D]$ for dipole and quadrupole modes of the particle with size $q = 1$ shown in the inset of (A).

we known, the natural width of the arbitrary resonance is given by the following expression[50]:

$$\gamma_l = \frac{q^{2l+1}(l+1)}{[l(2l-1)!!]^2(d\epsilon_D/d\omega)^l} \quad (17)$$

where the derivative $(d\epsilon_D/d\omega)^l$ is taken at the corresponding resonance frequency $\omega = \omega_l$. There is an extremely sharp decrease in γ_l with the increase of l . At the same time, the characteristic width γ_l will increase and the different resonance modes become to incorporate, following the increase of size q . As shown in the inset of Fig. 1A, the incorporation between dipole and quadrupole resonances induces that the quadrupole resonance still holds an important rule in scattering process even at $Im[\epsilon_D] = 0.3$ for the size $q = 1$. Whatever, we can find that the dipole resonance mode should be considered to be as an important role for the application of surface plasmons.

Since the small size is more effective for the surface plasmons as found in Fig. 1A and B, we will detect the giant resonance cross section in the size range $0 < q < 1$ for the small metal sphere. As the result of Rayleigh formula, the dipole scattering section increases quickly following ϵ_D reaches asymptotically the singular value -2 (in Fig. 2A) under the nondissipative limit, while the size q arrives at the limit value 0 from Mie theory as shown in Fig. 4A. With the dissipative damping, the resonance frequency of the maximal resonance cross section will have a large change, though the resonance frequency is just with an inconspicuous change by following the increase of $Im[\epsilon_D]$ at fixed size q . As Fig. 2A shown, the maximal resonance frequency has a red-shift with the decrease of the maximal cross section as a function of $Im[\epsilon_D]$. This means the maximal resonance scattering should be appeared on a particle with a limited small size and not on a particle with $q \rightarrow 0$.

Near plasmon resonance frequencies, the anisotropy of permittivity can lead to an additional increase in field enhancement has been shown. In Fig. 3A, the maximal scattering sec-

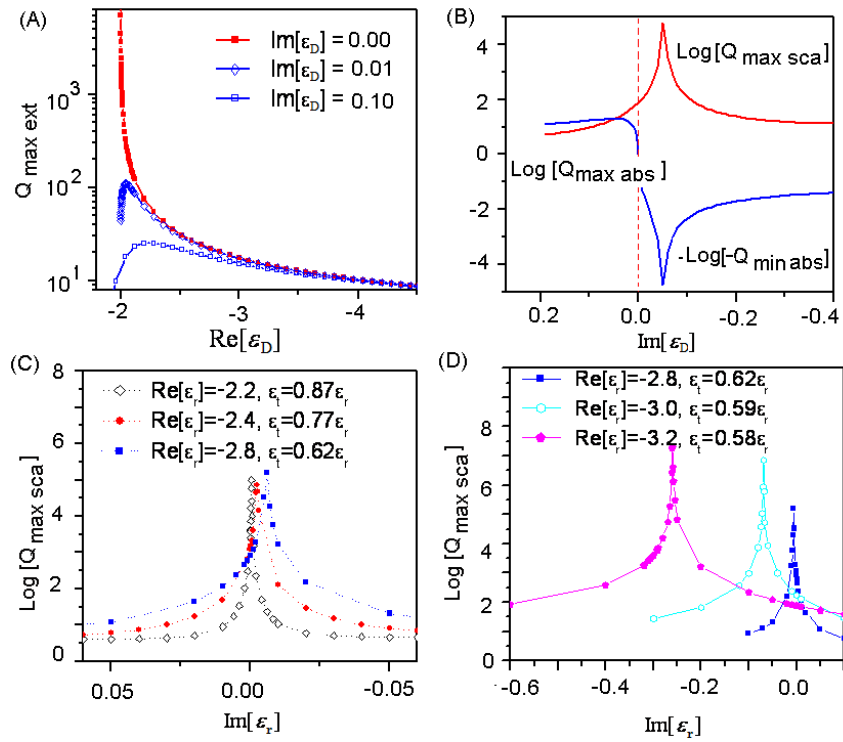


Fig. 2. The maximal value of Q_{ext} as a function of $Re[\epsilon_D]$ with different $Im[\epsilon_D]$ (A), the maximal or minimal values of Q_{sca} and Q_{abs} as a function of $Im[\epsilon_D]$ with $Re[\epsilon_D] = -2.2$ (B), maximal value of Q_{ext} as a function of $Im[\epsilon_r]$ with different $Re[\epsilon_r]$ and the ratio ϵ_i/ϵ_r (C and D).

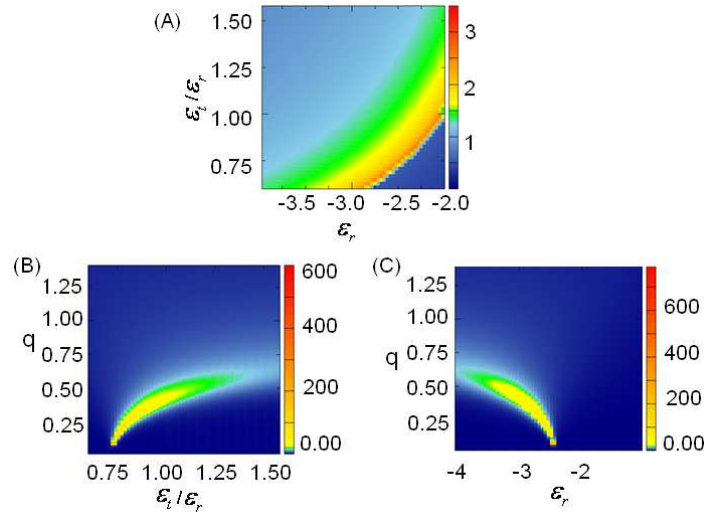


Fig. 3. $\text{Log}[Q_{max\ ext}]$ as a function of both ϵ_r and ϵ_i/ϵ_r (A), Q_{ext} as a function of q and ϵ_i/ϵ_r with fixed longitudinal permittivity $\epsilon_r = -2.5$ (B) and Q_{ext} as a function of q and ϵ_r with fixed ratio $\epsilon_i/\epsilon_r = 0.75$ (C), with the nondissipative limit ($Im[\epsilon_r] = 0$ and $Im[\epsilon_i] = 0$).

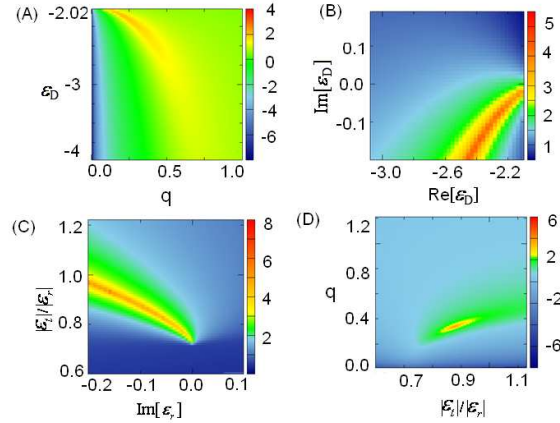


Fig. 4. $\text{Log}[Q_{ext}]$ as a function of permittivity ϵ_D and size q under the nondissipative limit ($\text{Im}[\epsilon_D] = 0$) (A), the maximal value of $\text{Log}[Q_{ext}]$ as a function of $\text{Re}[\epsilon_D]$ and $\text{Im}[\epsilon_D]$ (B), the maximal value of $\text{Log}[Q_{sca}]$ as a function of $\text{Im}[\epsilon_r]$ and the ratio $|\epsilon_t|/|\epsilon_r|$ for $\text{Re}[\epsilon_r] = -2.5$ and $\epsilon_t = (-2.5 + i \text{Im}[\epsilon_r])|\epsilon_t|/|\epsilon_r|$ (C), $\text{Log}[Q_{sca}]$ as a function of the ratio $|\epsilon_t|/|\epsilon_r|$ and size q for $\epsilon_r = -2.5 - 0.1i$ and $\epsilon_t = (-2.5 - 0.1i)|\epsilon_t|/|\epsilon_r|$ (D).

tion $Q_{max\ ext}$ as a function of both ϵ_r and ϵ_t/ϵ_r is demonstrated under the nondissipative limit ($\text{Im}[\epsilon_r] = 0$ and $\text{Im}[\epsilon_t] = 0$). It can be found that the maximal value of $Q_{max\ ext}$ will exist at the relative small ratio of ϵ_t to ϵ_r with the decrease of ϵ_r . Since the scattering efficiencies are inversely proportional to q^2 , the change of $Q_{max\ ext}$ following the change of the ratio ϵ_t/ϵ_r may be due to the shift in the resonance positions. As Fig. 3B shown, the maximal value of Q_{ext} is at the small size q with the decrease of the ratio ϵ_t/ϵ_r . Furthermore, the Q_{ext} also increases with the decrease of q and increase of ϵ_r at fixed ratio $\epsilon_t/\epsilon_r = 0.75$ shown in Fig. 3C. Therefore, the enhancement of resonance scattering efficiencies can be attributed mostly to the decrease of the size q .

As we shown, the resonance scattering section decreases quickly with the enhancement of the dissipative damping. If an assumed active mechanism with the negative value for $\text{Im}[\epsilon_D]$ is introduced, whether the scattering efficiency can increase need to be checked further. In Fig. 2B, the resonance cross sections of scattering ($Q_{max\ sca}$) and absorption ($Q_{min\ abs}$ or $Q_{max\ abs}$) as the functions of $\text{Im}[\epsilon_D]$ with the fixed $\text{Re}[\epsilon_D] (= -2.2)$ are analyzed. we find that $Q_{max\ sca}$ has a maximal value at the point with $\text{Im}[\epsilon_D] = -0.05$. At the same time, there is a minimal value for $Q_{min\ abs}$. It is well known that the absorption is attributed to the dissipative damping. With the decrease of $\text{Im}[\epsilon_D]$, the efficiency of absorption decreases, whereas the resonance scattering cross section increases. Thus, there is a maximal value for Q_{abs} at special point of $\text{Im}[\epsilon_D]$. At the limit of small size parameter, the maximal value of Q_{abs} is given by $Q_{abs\ max}^l = \frac{1}{q^2}(l + 1/2)$ [52]. Then at the nondissipative limit, the absorption cross section (Q_{abs}) will become zero. The negative Q_{sca} at the negative $\text{Im}[\epsilon_D]$ means the particle can emit light with some active mechanism. Therefore, the minimal value of $Q_{min\ abs}$ at $\text{Im}[\epsilon_D] = -0.05$ means there is light emitting with special resonance mechanism. In Fig. 4B, the $Q_{max\ sca}$ as the function of both $\text{Re}[\epsilon_D]$ and $\text{Im}[\epsilon_D]$ is shown. It is found that the maximal resonance scattering cross section exists with the more negative value of $\text{Im}[\epsilon_D]$ for the smaller $\text{Re}[\epsilon_D]$. In Fig. 2 C, D and Fig. 4 C, we demonstrate that the anisotropy of permittivity with different negative image part may result in the more large resonance cross sections of scattering and emitting. In Fig. 4D, we found that the giant resonance cross section is located at the region of special particle size.

In practice, the active metal is impossible to exist, since the overlap of valance band and

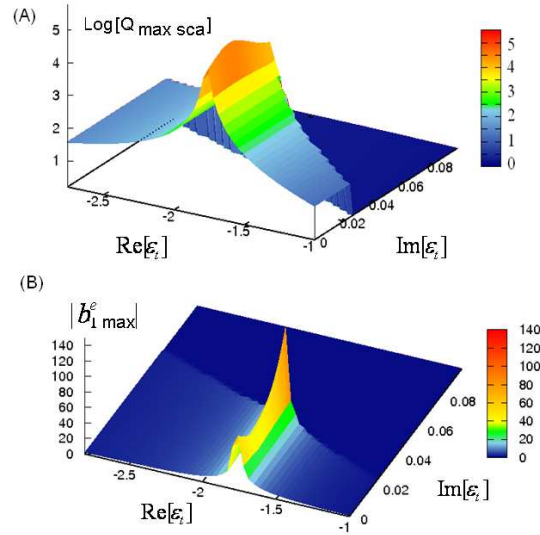


Fig. 5. the resonance cross section $\text{Log}[Q_{sca}]$ as a function of transverse permittivity ($\text{Re}[\epsilon_t]$ and $\text{Im}[\epsilon_t]$) with the fixed longitudinal permittivity $\epsilon_r = 2.5 - 0.05i$ (A), the maximal value of scattering amplitude $|b_1^e|$ as a function of $\text{Re}[\epsilon_t]$ and $\text{Im}[\epsilon_t]$ with the fixed $\epsilon_r = 2.5 - 0.05i$ (B).

conduction band at the Fermi level will result in an impotent radiation transition for any visible light and the energy gain from the model of absorption-emission can not be realized. However, if the dielectric or insulate, such as silica, is introduced in the system, the light absorption-emission model can be used to be as the mechanism of energy gain. Therefore, the active mechanism can be introduced by the anisotropic permittivity with ϵ_r or ϵ_t for the active medium. Then it is expected that the light gain can be coupled with the collective moving of electrons from metal. The giant resonance cross section for light scattering and adsorption (or emission) will be possible to be obtained.

For the metal particle, the giant scattering resonance cross section due to the surface plasmons is localized at the small size with $q < 1$. For dielectric particle, there isn't the ability to trap the electromagnetic field which results in the scattering cross section is small in the nano size for visible light. Since the surface plasmons mechanism is more effective for small size, we will limit the size of the anisotropic spherical particle in the region of $0 < q \leq 2$. As Fig. 5A shown, the maximal value of Q_{sca} is as a function of $\text{Re}[\epsilon_t]$ and $\text{Im}[\epsilon_t]$ with fixed longitudinal permittivity $\epsilon_r = 2.5 - 0.05i$. We can found that there is a region with $\text{Re}[\epsilon_t] \sim -1.8$ for giant scattering cross section duo to the resonance. It is known that the resonance from the electric dipole mode needs $\epsilon \leq -2$ for metal particle. Therefore, it is possible that there is a relation for both ϵ_r and ϵ_t in the region of resonance. It is also found that $\text{Im}[\epsilon_t]$ is less than 0.05 for the region of resonance. It seems that the energy gain from the active dielectric part (ϵ_r) must be larger than the dissipative damping from the metal part (ϵ_t) for the giant resonance cross section.

Is it possible that the giant resonance cross section is from the contribution of different scattering modes? After the analysis of scattering cross section, it is found that the electronic dipole mode is the major contribution for the special anisotropic particle with the size $0 < q \leq 2$. In Fig. 5B, the absolute value of the scattering amplitude b_1^e from electric dipole mode as a function of $\text{Re}[\epsilon_t]$ and $\text{Im}[\epsilon_t]$ with fixed longitudinal permittivity $\epsilon_r = 2.5 - 0.05i$ is shown. It

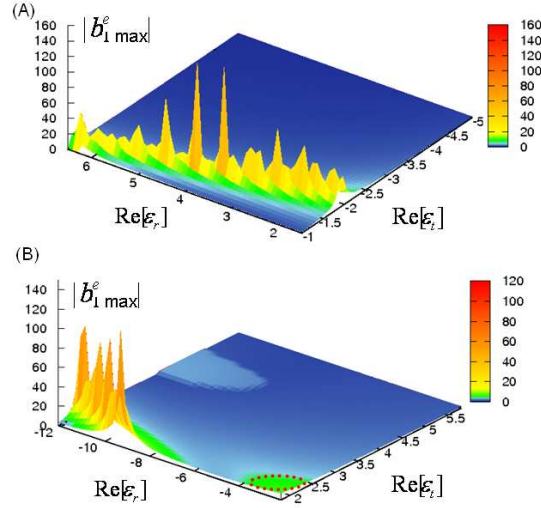


Fig. 6. the maximal value of scattering amplitude $|b_1^e|$ as a function of $Re[\epsilon_r]$ and $Re[\epsilon_t]$ with fixed $Im[\epsilon_r](= -0.05)$ and $Im[\epsilon_t](= 0.008)$ for ϵ_r as active medium (A), with fixed $Im[\epsilon_r](= 0.001)$ and $Im[\epsilon_t](= -0.02)$ for ϵ_t as active medium (B).

demonstrates the major contribution of electronic dipole mode. Therefore, it is considered that the electronic dipole mode will be possible to be the effective major mode to couple with the active medium for the particle with size $0 < q \leq 2$. Firstly, the longitudinal permittivity ϵ_r as the active medium is considered to be contributed to the the giant scattering cross section. In Fig. 6A, $|b_1^e|_{max}$ as a function of $Re[\epsilon_r]$ and $Re[\epsilon_t]$ with fixed image parts $Im[\epsilon_r] = 0.05$ and $Im[\epsilon_t] = -0.008$ is shown. Obviously, there is a quasi-linear region for the resonance cross section. By fitting the extremum of $|b_1^e|_{max}$ about $Re[\epsilon_r]$ and $Re[\epsilon_t]$, we find there is a quasi-linear relation ($Re[\epsilon_t] = -2.62 + 0.608Re[\epsilon_r] - 0.110Re[\epsilon_r]^2 + 0.008Re[\epsilon_r]^3$) for resonance region. Secondly, the transverse permittivity ϵ_t is considered to be as the active medium for the giant scattering cross section. In Fig. 6B, $|b_1^e|_{max}$ as a function of $Re[\epsilon_r]$ and $Re[\epsilon_t]$ with fixed image parts $Im[\epsilon_r] = 0.001$ and $Im[\epsilon_t] = -0.02$ is shown. It is found that there is also a linear relation about $Re[\epsilon_r]$ and $Re[\epsilon_t]$ for the resonance region. By fitting the value of $|b_1^e|_{max}$, the linear relation, $Re[\epsilon_t] = 0.389 - 0.154Re[\epsilon_r]$, is found.

With the relation about the real parts of both ϵ_r and ϵ_t , we can detect the dependence of the size about the resonance cross section in the resonance region in detail. From Fig. 7A and B, it is found that the size for resonance cross section changes with the real part of permittivity. Furthermore, by the relation of $Re[\epsilon_r]$ and $Re[\epsilon_t]$, the size is more dependent to the permittivity with the dielectric property. Then we can explore the dependence of resonance cross section to the dissipative damping from metal and the gain energy of active dielectric. Considering the weak dissipative limit, we just analyze the $Im[\epsilon_t]$ or $Im[\epsilon_r]$ in the region $[0, 0.3]$ for the damping. As shown in Fig. 7C and D, there is the special relation between $Im[\epsilon_t]$ and $Im[\epsilon_r]$ for the resonance process. It gives us an amazed conclusion that it is not the case that larger energy gain results in a stronger coupling to surface plasmons and then a larger resonance cross section. In additional, with the special ratio of $Im[\epsilon_t]$ and $Im[\epsilon_r]$, there are the giant resonance cross sections, such as for backscattering shown in Fig. 8. The giant cross sections should be attributed to the the resonance of electric dipole mode with the assistance of gain energy from the active ϵ_r or ϵ_t and this maybe result in spaser.

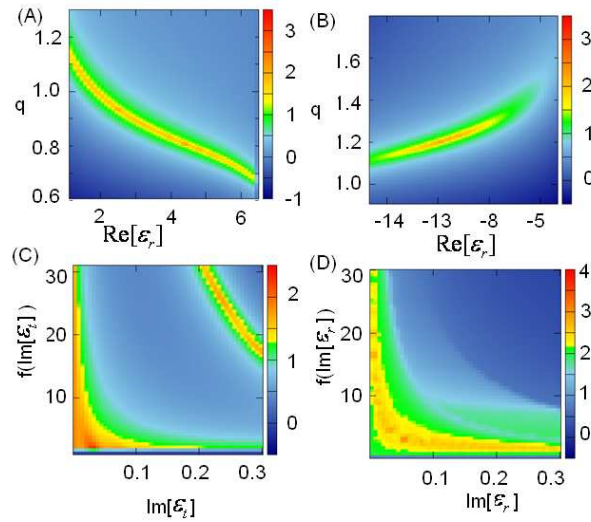


Fig. 7. the scattering amplitude $\text{Log}[|b_1^e|]$ as a function of $\text{Re}[\epsilon_r]$ and q with fixed $\text{Im}[\epsilon_r](= -0.05)$ and $\text{Im}[\epsilon_t](= 0.008)$ ($\text{Re}[\epsilon_t]$ is chosen by the formula $\text{Re}[\epsilon_t] = -2.62 + 0.608\text{Re}[\epsilon_r] - 0.110\text{Re}[\epsilon_r]^2 + 0.008\text{Re}[\epsilon_r]^3$)(A), the scattering amplitude $\text{Log}[|b_1^e|]$ as a function of $\text{Re}[\epsilon_r]$ and q with fixed $\text{Im}[\epsilon_r](= 0.001)$ and $\text{Im}[\epsilon_t](= -0.02)$ ($\text{Re}[\epsilon_t]$ is chosen by the formula $\text{Re}[\epsilon_t] = 0.389 - 0.154\text{Re}[\epsilon_r]$)(B), the maximal value of scattering amplitude $\text{Log}[|b_1^e|]$ as a function of $f(\text{Im}[\epsilon_r])$ and $\text{Im}[\epsilon_r]$ with $\epsilon_r = 3 - f(\text{Im}[\epsilon_r])\text{Im}[\epsilon_r]i$ and $\text{Re}[\epsilon_t] = -1.5604$ (C) and the maximal value of scattering amplitude $\text{Log}[|b_1^e|]$ as a function of $f(\text{Im}[\epsilon_r])$ and $\text{Im}[\epsilon_r]$ with $\text{Re}[\epsilon_r] = -12$ and $\epsilon_t = 2.237 - f(\text{Im}[\epsilon_r])\text{Im}[\epsilon_r]i$ (D).

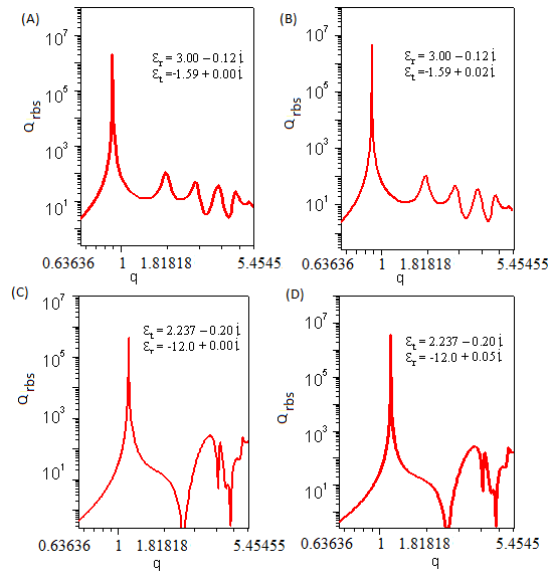


Fig. 8. High scattering efficiencies with huge radar backscattering cross section. Q_{rbs} as the function of size q for ϵ_r with the property of energy-gain (A and B) and for ϵ_t with the property of energy-gain (C and D).

4. Conclusion

With the expanded Mie theory, the Maxwell's equations are solved by the Debye's scalar potentials and the electromagnetic fields are expressed in terms of Bessel functions with Legendre functions. Thus, the light scattering of spherical structure with anisotropic permittivity can be analyzed effectively. For metal particle, small dissipative damping will result in the rapid decrease of resonance scattering cross section. Furthermore, the resonance cross section of higher order scattering mode decreases more quickly than that of dipole mode. This explains that why the electric dipole approximation is an effective method for small metal particle, and it also implies that the dipole mode may be an effective way to control light energy into nanometer scale.

With designing the transverse permittivity ϵ_t and the longitudinal permittivity ϵ_r , we can introduce an active mechanism to compensate the damping dissipation of plasmons and even enhance the resonance of plasmons. With the analysis of extinction, scattering, absorption and radar cross section, the electric anisotropy effects on scattering efficiency are studied systematically for small particle. Following the change of the transverse permittivity ϵ_t , the longitudinal permittivity ϵ_r and the particle size q , the huge scattering cross sections are found at the regions with special parameters. The huge cross sections are considered to be due to the coupling between the surface plasmon with electric dipole mode and the active medium. This coupling results in the strong light emitting and scattering.